PS-12-9

Extended Abstracts of the 2013 International Conference on Solid State Devices and Materials, Fukuoka, 2013, pp392-393

Structural and transport properties in epitaxial $Fe_2CrSi/MgAl_2O_x/Fe_2CrSi$ structures

Keima Inagaki[1], Naoto Fukatani[1], Hidekazu Tanaka[1], Tetsuya Miyawaki[1], Kenji Ueda[1], and Hidefumi Asano[1]

[1] Nagoya Univ.
Furo-cho, Chikusa-ku, Nagoya 464-8603, Japan
Phone: +81-52-789-3570 E-mail: miyawaki@numse.nagoya-u.ac.jp

Abstract

The structural and transport properties in $Fe_2CrSi/MgAl_2O_x/Fe_2CrSi$ were studied. Full-epitaxial $Fe_2CrSi/MgAl_2O_x/Fe_2CrSi$ structures were obtained. From the differential conductance measurements, the combination of protective $MgAl_2$-oxidation layer and reactively sputtered $MgAl_2O_x$ layer show potential properties for suitable tunnel barriers for MTJs.

1. Introduction

Magnetic tunnel junctions (MTJs) using the combination of epitaxial MgO barriers and half-metallic Heusler alloys have widely been used since they exhibit large tunnel magnetoresistance (TMR) ratios. However, misfit dislocations and antisite disorder at interfaces between the MgO and Heusler alloys induced by the large mismatch (about 4%) drastically reduce device performance[1].

$MgAl_2O_4$ is a candidate for the lattice-matched material for MTJs, since the lattice mismatch between $MgAl_2O_4$ and typical half-metallic Heusler alloys is less than 1%[2,3]. Although the reactive sputtering is a suitable method for the epitaxial growth of $MgAl_2O_x$[4], recent study showed that the conductance properties of $MgAl_2O_x$ barrier was mediated by the oxygen vacancy[4]. Here, we report the improved transport properties of $MgAl_2O_x$ tunnel barrier fabricated by the combined method of the reactive sputtering and the post-oxidation of metal $MgAl_2$. Also, using this method, full-epitaxial structures consist of half-metallic Heusler alloy as both the bottom and top electrodes were obtained for the first time for $MgAl_2O_4$-based MTJs. Heusler alloy Fe_2CrSi was used as the electrodes. A robustness of the high spin polarization of Fe_2CrSi against disorder and temperature is predicted due to a large DOS of majority spins at the Fermi energy.

2. Experimental

Multilayer structures consisting of $Fe_2VSi(5)/Fe_2CrSi(20)/MgAl_2(t_1)$-oxidation/$MgAl_2O_x(t_2)/Fe_2CrSi(20)$ were prepared on (001)$MgAl_2O_4$ or (001) MgO substrates by the magnetron sputtering method. Fe_2VSi layer was used as a buffer layer. After the deposition of Fe_2CrSi at room temperature, Fe_2CrSi was annealed at 500 °C. $MgAl_2O_x$ layer of t_2 was fabricated by the reactive sputtering method[4]. Since the reactive sputtering is conducted in the oxygen atmosphere, in order to prevent surface oxidation of the bottom Fe_2CrSi layer, thin protective layer of t_1 nm was fabricated by metal $MgAl_2$ deposition and post-oxidation method before the reactive sputtering. The protective layer was fabricated as follows. Firstly, $MgAl_2$ was deposited at room temperature in Ar atmosphere, followed by the introduction of pure oxygen gas into the chamber to oxidize the $MgAl_2$ layer. Typical oxygen pressure was 10 Torr. Subsequently, the reactive sputtering of $MgAl_2O_x$ was conducted at 300 °C. The typical pressure of Ar+10~20% O_2 for the reactive sputtering was 70 mTorr. Finally, Fe_2CrSi for the top electrode was deposited at 500 °C. We also fabricated $Fe_2CrSi(20)/MgAl_2(t_1)$-oxidation/NiFe(20) structures to optimize the fabrication conditions for the protective layer. In order not to affect the structural and transport properties of the barrier during the deposition of the top electrodes, NiFe electrodes deposited at room temperature were used in these structures. X-ray diffraction (XRD) with Cu K_α radiation was used for the structural characterization. Magnetic hysteresis loops of continuous films were measured by vibrating sample magnetometry (VSM). Conventional four-terminal method was used to study the conductance properties.

3. Results and discussions

The post-oxidized $MgAl_2$ protective layer should be a continuous film without pinholes, in order to prevent oxidation of the bottom Fe_2CrSi surface during the reactive sputtering of the tunnel barrier. The differential conductance properties (dI/dV) were measured to investigate the quality of the protective layer. Figure 1 (a) shows the normalized dI/dV curves for the $Fe_2CrSi(10)/MgAl_2(1.8)$-oxidation/NiFe(20) sample. The dI/dV curves at 4.2 K and 300 K show only slight bias dependence. Also, the difference in dI/dV values between 4.2 K and 300 K are almost equal at each bias level. These features are the typical characteristics for the junctions where the ohmic conductance cannot be neglected, which might be resulted from pinholes due to the small thickness[5]. The inset of Fig. 1(a) shows the resistance area product (RA) as a function of t_1. The RA values remain small for t_1 below 2.0 nm, while that for t_1 = 2.2 nm shows significant increase. In Fig. 2(b), the sample with t_1 = 2.2 nm, the significant suppression of the conductance at low bias levels is observed. Also, the difference in the dI/dV values between 4.2 K and 300 K is more pronounced with lowering the bias voltage. These

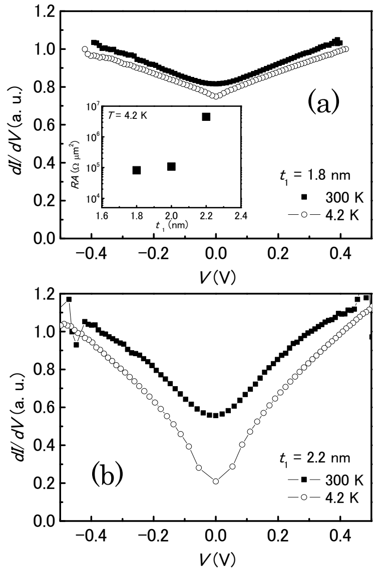

Fig. 1. Differential conductance curves for $Fe_2CrSi(10)/MgAl_2$ (t_1)-oxidation/NiFe(20) structures. (a) t_1 = 1.8 nm, (b) t_1 = 2.2 nm. All the dI/dV values are normalized by the dI/dV at 0.4 V at 4.2 K.

results suggest that the tunneling conduction plays a major role in this sample with t_1 = 2.2 nm[5]. Thus, we decided the thickness of the protective layer to 2.2 nm.

Figure 2(a) shows a XRD θ-2θ scan for $Fe_2CrSi(20)/MgAl_2(2.2)$-oxidation/$MgAl_2O_4/Fe_2CrSi(20)$ structure fabricated on a (001) MgO substrate. Only the (002) and (004) peaks of Fe_2CrSi and a (004) peak of $MgAl_2O_4$ are visible without any other orientations. Combining this data with the results of in-plane ϕ scans (not shown here), epitaxial $Fe_2CrSi/MgAl_2O_4/Fe_2CrSi$ structure was obtained. Figure

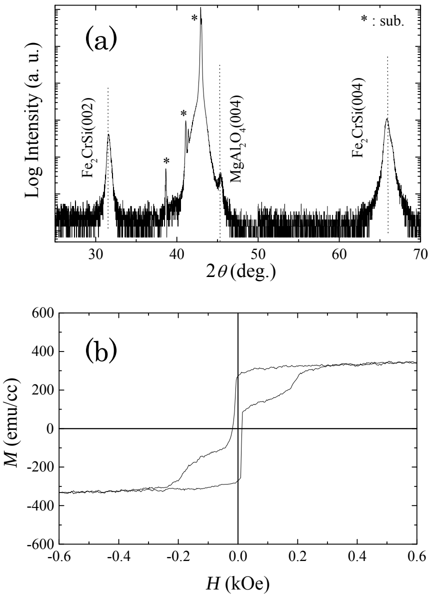

Fig. 2 (a) The XRD θ-2θ scan of $Fe_2CrSi(20)/MgAl_2(2.2)$- oxidation/$MgAl_2O_4(2.0)/Fe_2CrSi(20)$ structure. (b) The *M-H* curve for the same structure in (a).

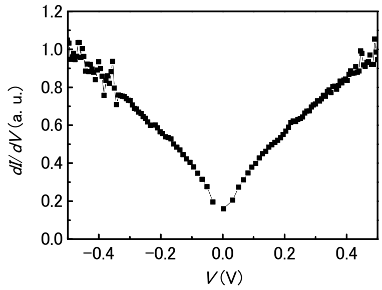

Fig. 3. The normalized differential conductance curve for Fe_2CrSi (10)/$MgAl_2$ (2.2)-oxidation/$MgAl_2O_x(2.0)/Fe_2CrSi(20)$ structure.

2(b) shows the *M-H* curve for the $Fe_2CrSi(20)/MgAl_2(2.2)$-oxidation/$MgAl_2O_4/Fe_2CrSi(20)$ structure. Clear two-step hysteresis loop is obtained, indicating that the both top and bottom Fe_2CrSi electrodes have good ferromagnetic properties. As shown in Fig. 3, the differential conductance curve for the Fe_2CrSi (10)/$MgAl_2(2.2)$-oxidation/$MgAl_2O_x$ (2.0)/$Fe_2CrSi(20)$ suggests that the tunnel conduction dominates the transport property of this barrier. The obtained barrier height from the fitting using Simmons' model[6] was ~0.8 eV, which is comparable to the value expected from the work functions of the electrodes and the barrier layers, contrary to the value ~0.15 eV for the tunnel conduction mediated by the oxygen vacancy[4]. The *dI/dV* values show the symmetric behavior about zero bias voltage, suggesting that the both interfaces between the barrier and top/bottom electrodes have the same quality. These results suggest that the insertion of the oxidized protective layer is highly effective not only to prevent from the oxidation of the bottom Fe_2CrSi layer, but also for the epitaxial growth and the improvement of the tunnel conductance properties in $MgAl_2O_4$-based MTJs.

3. Conclusions

In this paper, the structural and conductance properties in $Fe_2CrSi/MgAl_2O_x/Fe_2CrSi$ were studied. Full-epitaxial $Fe_2CrSi/MgAl_2O_x/Fe_2CrSi$ structures were obtained. The combination of protective $MgAl_2$-oxidation layer and reactively sputtered $MgAl_2O_x$ layer provides lattice-matched, pinhole-free tunnel barrier for the MTJs based on half-metallic Heusler alloys.

References

[1] T. Miyajima, M. Oogane, Y. Kotaka, T. Yamazaki, M. Tsukada, Y. Kataoka, H. Naganuma, and Y. Ando, Appl. Phys. Express **2** (2009) 093001.

[2] N. Fukatani, C. Shishikura, Y. Takeda, and H. Asano, Appl. Phys. Express **2** (2009) 053001.

[3] H.Sukegawa, H. Xiu, T. Ohkubo, T. Furubayasi, T. Niizeki, W. Wang, S. Kasai, S. Mitani, K. Inomata, and K. Hono, Appl. Phys. Lett. **96** (2010) 212505.

[4] K. Inagaki, N. Fukatani, K. Mari, H. Fujita, T. Miyawaki, K. Ueda, and H. Asano, J. Korean Phys. Soc., *accepted*.

[5] J. J. Åkerman, J. M. Slaughter, R. W. Dave, and I. K. Schuller, Appl. Phys. Lett. **79** (2001) 3014.

[6] J. G .Simmons, J. Appl. Phys. **34** (1963) 1793.